Collectivity of light Ge and As isotopes

A. Corsi,[1] J.-P. Delaroche,[2] A. Obertelli,[1] T. Baugher,[3,4] D. Bazin,[4] S. Boissinot,[1] F. Flavigny,[1] A. Gade,[3,4] M. Girod,[2] T. Glasmacher,[3,4] G. F. Grinyer,[5] W. Korten,[1] J. Libert,[2] J. Ljungvall,[1,*] S. McDaniel,[3,4] A. Ratkiewicz,[3,4] A. Signoracci,[1] R. Stroberg,[3,4] B. Sulignano,[1] and D. Weisshaar[4]

[1]*CEA, Centre de Saclay, IRFU/Service de Physique Nucléaire, F-91191 Gif-sur-Yvette, France*
[2]*CEA, DAM, DIF, F-91297 Arpajon, France*
[3]*Michigan State University, East Lansing, Michigan 48824, USA*
[4]*National Superconducting Cyclotron Laboratory, East Lansing, Michigan 48824, USA*
[5]*Grand Accélérateur National d'Ions Lourds (GANIL), CEA/DSM-CNRS/IN2P3, Boulevard Henri Becquerel, 14076 Caen, France*

(Received 25 July 2013; published 11 October 2013)

Background: The self-conjugate nuclei of the $A \sim 70$ mass region display rapid shape evolution over isotopic or isotonic chains. Shape coexistence has been observed in Se and Kr isotopes reflecting the existence of deformed subshell gaps corresponding to different shell configurations. As and Ge isotopes are located halfway between such deformed nuclei and the $Z = 28$ shell closure.

Purpose: The present work aims at clarifying the low-lying spectroscopy of ^{66}Ge and ^{67}As, and providing a better insight into the evolution of collectivity in light even-even Ge and even-odd As isotopes.

Methods: We investigate the low-lying levels and collectivity of the neutron deficient ^{67}As and ^{66}Ge through intermediate-energy Coulomb excitation, inelastic scattering, and proton knockout measurements. The experiment was performed using a cocktail beam of ^{68}Se, ^{67}As, and ^{66}Ge nuclei at an energy of 70–80 MeV/nucleon. Spectroscopic properties of the low-lying states are compared to those calculated via shell model with the JUN45 interaction and beyond-mean-field calculations with the five-dimensional collective Hamiltonian method implemented using the Gogny D1S interaction. The structure evolution of the lower-mass Ge and As isotopes is discussed.

Results: Reduced electric quadrupole transition probabilities $B(E2)$ have been extracted from the Coulomb-excitation cross sections measured in ^{66}Ge and ^{67}As. The value obtained for the $B(E2; 0_1^+ \rightarrow 2_1^+)$ in ^{66}Ge is in agreement with a recent measurement, ruling out the existence of a minimum at $N = 34$ in the $B(E2)$ systematics as previously observed. New transitions have been found in ^{67}As and were assigned to the decay of low-lying negative-parity states.

DOI: 10.1103/PhysRevC.88.044311 PACS number(s): 21.10.Ky, 25.70.De, 23.20.Lv, 27.50.+e

I. INTRODUCTION

The rapid evolution of nuclear deformation is a subtle feature which stems from the quantum nature of the atomic nucleus, whose macroscopic properties can drastically change when adding or removing a few nucleons. While most of the open-shell nuclei are collective and deformed, the competition between oblate and prolate quadrupole shapes close to the ground state has been predicted and observed only in few regions of the nuclear chart [1,2]. One of them is the region of light Kr and Se isotopes with $N \sim Z$. A transition from a prolate to an oblate shape has been observed along the Kr isotopic chain between $N = 34$–36 and $N = 32$ [3,4]. The same occurs along the Se isotopic chain between $N = 38$ and $N = 34$–36 [5,6]. In the first case the shape transition is associated with shape coexistence in $^{74-76}$Kr [4,7,8].

Below Se, the Ge isotopes represent an intermediate case between the well deformed Se, Kr, and Sr and the spherical nuclei close to the $Z = 28$ shell closure. The onset of collectivity associated with the filling of the $f_{5/2}pg_{9/2}$ shell (between the $N = Z = 28$ and the $N = Z = 50$ magic numbers) was described in Refs. [9,10] using the systematics of the $B(E2; 0_1^+ \rightarrow 2_1^+)$'s [$B(E2\uparrow)$ in the following] for $N = Z$ nuclei from ^{60}Zn to ^{76}Sr. For these neutron-deficient nuclei the quadrupole moment of low-lying excited states (directly related to their charge distribution) is experimentally not accessible today. The measurement of $B(E2\uparrow)$'s [or, equivalently, $B(E2\downarrow)$'s] is one way to probe their collective properties and, via model comparison, their shape. The measured $B(E2\uparrow)$'s are compatible with a transition from a moderately prolate shape in ^{60}Zn to an oblate shape in ^{72}Kr, passing through triaxial shapes in ^{64}Ge [11] and ^{68}Se [9].

The rich information gained from measurements collected over the past 40 years points to complex spectroscopic properties for $A \sim 70$–80 nuclei. There are strong indications for collective and noncollective modes coming into play and interweaving in the low-energy spectra of Ge isotopes near $N = 40$. A systematic study of Coulomb excitation measurements for even-even Ge isotopes suggests that two structures, one spherical and the other deformed, coexist in one nucleus and reach maximum mixing in ^{72}Ge [12,13]. A similar scenario based on the shell-model picture was discussed in Ref. [2]. For other publications dedicated to various facets of the interplay between collective and noncollective degrees of freedom in this mass region, see [14–27].

Two neutrons and two protons away from the $N = Z$ line, ^{66}Ge presented an anomalously low value of $B(E2\uparrow)$ [28]

*Present address: CSNSM-IN2P3-CNRS, 91405 Orsay, France.

with respect to its neighbor isotopes and isotones and to shell-model predictions [29]. This $B(E2\uparrow)$ value has been remeasured independently at Yale via the recoil distance Doppler shift (RDDS) technique [30] and in the present work at the National Superconducting Cyclotron Laboratory (NSCL) via intermediate-energy Coulomb excitation. The Yale measurement uses the same technique as in Ref. [28], but the lifetime of the 2^+_1 state was extracted from the spectrum gated on the $4^+_1 \to 2^+_1$ transition. The possibility of analyzing the data by using γ-γ coincidences allows us to exclude feeding from long-lived states above the measured 2^+_1. The RDDS measurement yields a value $B(E2;2^+_1 \to 0^+_1) =$ 16.9(22) W.u., higher than the previous value but still below theoretical predictions [29].

As in the case of even-even isotopes, $B(E2\uparrow)$'s of odd-even and odd-odd isotopes reflect collectivity and deformation properties. A transition from a prolate $3/2^-$ to an oblate $5/2^-$ ground state between ^{67}As and ^{65}As is predicted by beyond-mean-field calculations [31]. An inversion in the ground-state spin has been experimentally determined in a series of experiments [31–33]. The higher level density of odd-odd and odd-even nuclei makes the study of their spectroscopy and spin assignments more challenging. Except for a few experiments [31,34], the spectroscopy of neutron-deficient As isotopes has been studied only via fusion evaporation [32,33] which populates mainly high-spin states.

Direct probes, such as knockout reactions [35] and Coulomb excitation [36] bring valuable information on the low-lying spectroscopy of nuclei in this region. One-nucleon removal reactions allow one to probe the overlap between the wave function of the final state and that of the projectile ground state. Intermediate-energy Coulomb excitation strongly favors $E2$ multipolarity [37], and is a powerful tool to extract $B(E2\uparrow)$ transition probabilities from the ground state to low-lying excited states in exotic nuclei produced at low beam intensities.

We report here on the spectroscopy of two neutron-deficient $N = 34$ isotones, ^{66}Ge and ^{67}As, that were studied via a combination of Coulomb excitation, inelastic scattering, and knockout reactions. Results obtained in this same experiment for ^{66,68}Se and ^{65}As have already been published [9,31].

The paper is organized as follows. The experimental setup is briefly described in Sec. II. The data reduction together with shell- and collective-model analyses of present $B(E2)$ measurements are presented and discussed in Sec. III. The scope of the present study is next expanded in Sec. IV by challenging both model predictions for structure properties measured for the $^{64-72}$Ge isotopes. Properties of interest are spectroscopic quadrupole measurements of first and second 2^+ states, odd-even staggering of 2^+, 3^+, and 4^+ members of γ bands, and $B(E2)$ ratios for transitions between the second and first 2^+ levels and between the second 2^+ and ground-state 0^+ levels. Highlights on the key role played by collective masses in present collective model predictions are finally presented. Sec. V provides a summary of present experimental results as well as suggestions for new measurements. Improvements for structure model predictions are also suggested.

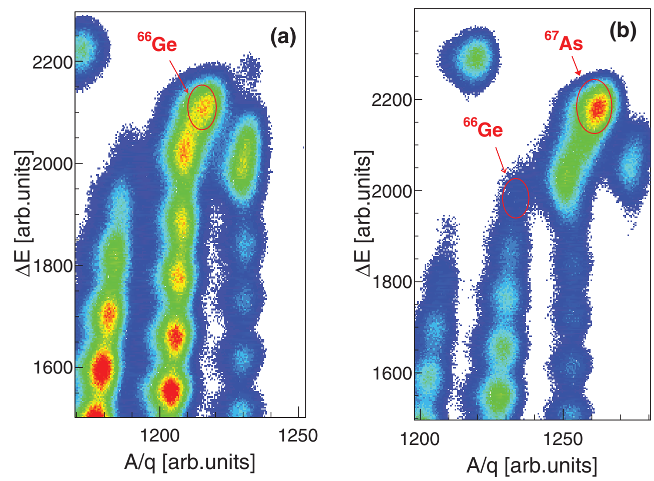

FIG. 1. (Color online) Identification of the isotopes produced in reaction from the ^{66}Ge beam (a) and the ^{67}As beam (b) impinging on a ^{9}Be target. The atomic number is given by the energy loss ΔE in the ionization chamber at the S800 focal plane and A/q by a time-of-flight measurement.

II. SETUP

Our experiment was performed at the National Superconducting Cyclotron Laboratory (NSCL) at Michigan State University. A cocktail beam of ^{68}Se (12%), ^{67}As (41%), and ^{66}Ge (30%) was produced by fragmentation of a ^{78}Kr primary beam at 150 MeV/nucleon on a 329 mg/cm^2 thick ^{9}Be production target. The secondary beam impinged on a 257 mg/cm^2 thick ^{197}Au target for Coulomb excitation and on a 188 mg/cm^2 thick ^{9}Be target. The energy of ^{66}Ge was 79 MeV/nucleon and 70 MeV/nucleon at the middle of the secondary ^{197}Au and ^{9}Be targets, respectively. The targets were placed at the pivot point of the S800 spectrometer [38] and surrounded by the segmented high-purity germanium array (SeGA) [39]. For this experiment, SeGA was composed of 17 detectors positioned at 20 cm from the target and arranged in a configuration of two rings in a cylindrical symmetry around the beam axis: 7 detectors at 37° in the forward direction and 10 detectors at 90° relative to the beam axis. The photopeak efficiency of the SeGA array was 2.49(2)% for a 1-MeV γ ray emitted at rest in the laboratory frame from the target position. Incoming particle identification was performed on an event-by-event basis by a time-of-flight measurement between two plastic scintillators located at the image point of the A1900 fragment separator [40] and at the object point of the S800 magnetic spectrometer. Outgoing particles were identified event-by-event via a correlation of the energy loss in the ionization chamber at the focal plane of the S800 spectrometer and the time of flight between a scintillator at the object point and at the focal plane of S800 (Fig. 1).

III. ANALYSIS

Coincidences between γ rays and incoming and outgoing particles have been measured. A time gate on prompt events has been applied to reduce random coincidences. The low-lying excited states of the isotopes under study, ^{66}Ge and ^{67}As, have been populated via Coulomb excitation, ^{9}Be-induced inelastic scattering, and one-proton knockout. For ^{67}As populated via one-proton knockout from ^{68}Se, the statistics in the γ-ray spectra were too low to observe transitions in coincidence. This is due to the fact that during the measurement with the ^{9}Be target the rigidity of the S800 magnetic spectrometer was tuned to optimize the two-neutron removal channel, which was the main goal of the experiment. The $B\rho$'s of the inelastic scattering and one-proton knockout products are 2.6% and 4.3% off, respectively, with respect to the central momentum of the spectrometer S800, 2.25 Tm. Therefore only part (for the inelastic scattering) or a tail of the momentum distribution (for the knockout reaction) was within the acceptance, preventing us from extracting absolute cross sections.

A. Spectroscopy of ^{66}Ge

The γ-ray spectra of ^{66}Ge are shown in Fig. 2. The velocities used in the Doppler correction are $\beta = 0.387$, 0.376, and 0.380 in the Coulomb-excitation, inelastic, and one-proton knockout channels, respectively. The use of different β values stems from the fact that the beam energy on the target was different for the two different targets (^{197}Au and ^{9}Be) and different isotopes in the same cocktail beam. Energies of the observed transitions are listed in Table I. They are consistent with the energies of the known transitions depopulating the 2_1^+, 4_1^+, and 2_2^+ states [28]. In the following, we will refer to the transitions with the centroid energy measured in the

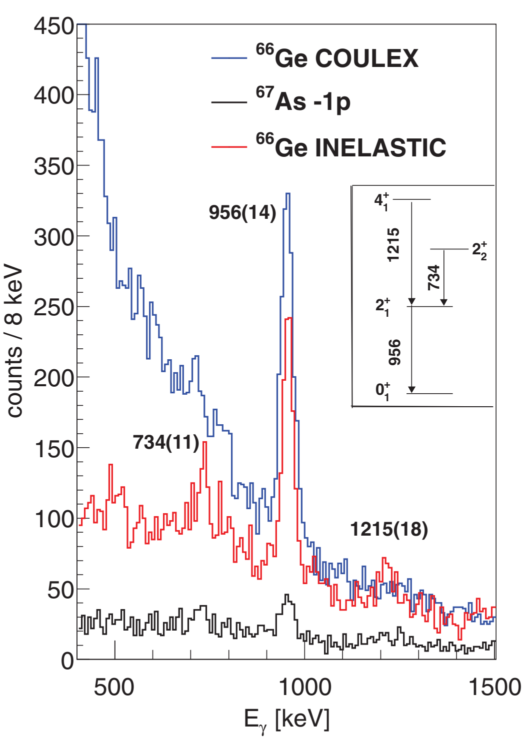

FIG. 2. (Color online) γ-ray spectra of ^{66}Ge. The spectra correspond to the decay of excited states populated in the inelastic (red), Coulomb excitation (blue), and one-proton knockout channels (black), respectively. The level scheme deduced from the observed transitions is plotted in the inset. Transition energies are given in keV.

TABLE I. Energies of the transitions measured in coincidence with ^{66}Ge. The errors are obtained as the quadratic sum of the error of the fit, the error due to an uncertainty of 0.005 on the value of β adopted in the Doppler correction, and a 4-keV error on the calibration.

J_i^π	E_{ex} [28] (keV)	Transition	E_γ^{coulex} (keV)	$E_\gamma^{\text{inelastic}}$ (keV)	E_γ^{-1p} (keV)
2_1^+	957.5(0.5)	$2_1^+ \to 0_1^+$	954(5)	956(5)	956(6)
4_1^+	2174.7(0.7)	$4_1^+ \to 2_1^+$		1215(5)	1214(9)
2_2^+	1694.0(0.5)	$2_2^+ \to 2_1^+$		734(5)	732(8)

inelastic scattering channel, where all of them are present. In the Coulomb excitation channel only the 2_1^+ state is populated. The γ-ray spectrum measured in this channel allows us to extract the transition probability $B(E2\uparrow)$ to the 2_1^+ state using the semiclassical theory of Alder and Winther for relativistic Coulomb excitation [41]. In the analysis, the cross sections were calculated for four different ranges of safe angles up to 3°. The results are shown in Fig. 3. The value obtained at 3° is not consistent since this angle is at the limit of the acceptance of the S800 spectrometer (3.5°). Therefore the final $B(E2\uparrow) = 1401(69)\ e^2\text{fm}^4$ is the average of the results obtained in the three angular ranges up to 2.5°.

A $B(E2; 2_2^+ \to 0_1^+) = 0.07^{+0.05}_{-0.02}$ W.u. was deduced by Wadsworth *et al.* [28], corresponding to $B(E2; 0_1^+ \to 2_2^+) = 5^{4}_{-2}\ e^2\text{fm}^4$ [42].

Taking into account the experimental branching ratio of 70% to the 2_1^+, we expect to observe only a few counts in the $2_2^+ \to 2_1^+$ transition around 734 keV. Such low statistics cannot be distinguished from background fluctuations and from the Compton edge of the 956 keV peak in our spectrum. Even fewer counts are expected based on shell-model predictions using the JUN45 interaction [29]. From our data and assuming that a peak of about 50 counts cannot be distinguished from background fluctuation, we can only deduce an upper limit of about 50 $e^2\text{fm}^4$ for the $B(E2; 0_1^+ \to 2_2^+)$ value.

The $B(E2\uparrow)$ extracted from this experiment is in good agreement with the result obtained by Luttke *et al.* [30],

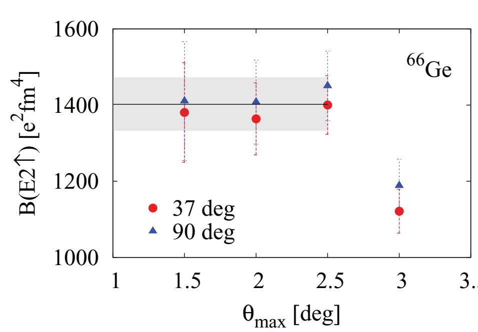

FIG. 3. (Color online) $B(E2\uparrow)$ transition probabilities for the $0_1^+ \to 2_1^+$ transition in ^{66}Ge. The red and blue points corresponds to the results obtained for the 37° and 90° ring with their statistical error. The black line corresponds to the average obtained considering the results up to 2.5°, and the shaded area represents the error on the average.

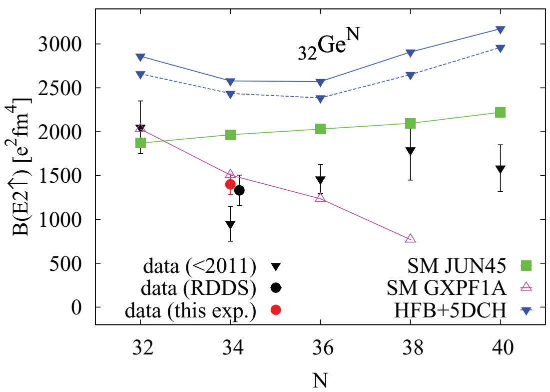

FIG. 4. (Color online) Experimental [11,48] and calculated $B(E2\uparrow)$'s for Ge isotopes from $N = 32$ to $N = 40$. The value for ^{66}Ge from Ref. [28] is presented together with the one obtained with the RDDS technique [30] and our result. The measured values are compared with those calculated with shell model using the JUN45 [29] and the GXPF1A [43] interactions, and with 5DCH calculations based on the Gogny D1S force [45]. The 5DCH predictions are displayed without (continuous blue curve) and with (dotted blue curve) renormalized collective masses. For more details, see Sec. IV E.

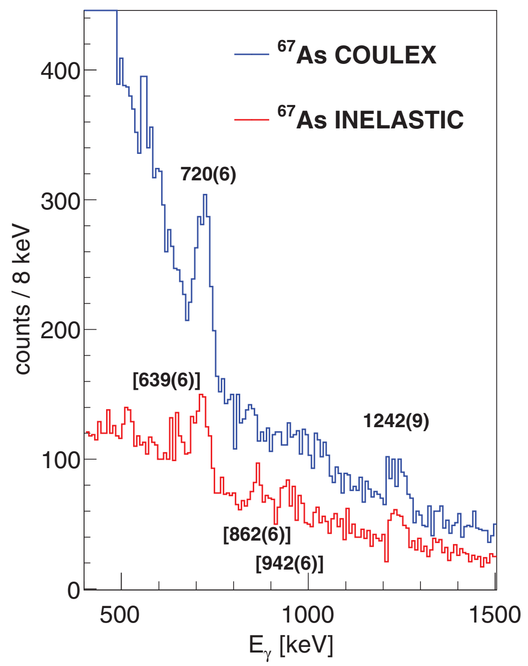

FIG. 5. (Color online) γ-ray spectra of ^{67}As. The red and blue lines correspond to the decay of excited states populated in the inelastic scattering and Coulomb excitation, respectively. Transition energies are given in keV and are between square brackets when no spin-parity assignment is can be argued based on the present data.

corresponding to $B(E2\uparrow) = 1339(174)\ e^2\mathrm{fm}^4$. We therefore agree on excluding the minimum in the $B(E2\uparrow)$ systematics obtained by Wadsworth *et al.* [28].

Shell-model calculations performed in the fp valence space (including the $f_{7/2}$, $p_{3/2}$, $f_{5/2}$, and $p_{1/2}$ orbitals) with the GXPF1A interaction [43] reproduce the experimental $B(E2\uparrow)$'s at $N = 32$, 34, 36 but fail at $N = 38$ [30]. Shell-model calculations in the $f_{5/2}pg_{9/2}$ model space (including the $p_{3/2}$, $p_{1/2}$, $f_{5/2}$, and $g_{9/2}$ orbitals) using the JUN45 interaction [29] predict a rather flat trend of the $B(E2\uparrow)$'s, similar to the experimental one (see Fig. 4). Compared to the experimental values, JUN45 calculations overestimate by 10%–40%. Calculations with the GXPF1A and JUN45 interaction were performed with the standard effective charges (1.5e for protons and 0.5e for neutrons) and with a higher neutron effective charge (1.1e), respectively, as prescribed in [29,43]. The occupation of the $g_{9/2}$ proton (neutron) orbital in ^{66}Ge is 0.2 (0.5) for the 0_1^+ and 2_1^+ states with the JUN45 interaction in the $f_{5/2}pg_{9/2}$ model space. The role of the $g_{9/2}$ orbital in the $f_{5/2}pg_{9/2}$ valence space may explain the missing collectivity resulting from a shell-model calculation performed in the fp model space, where the $g_{9/2}$ orbital is absent. The collectivity increase between ^{66}Ge and ^{64}Ge is not reproduced by shell-model calculations in the $f_{5/2}pg_{9/2}$ shell. This missing collectivity has been attributed to the lack of the $f_{7/2}$ orbit in the $f_{5/2}pg_{9/2}$ valence space [44].

We have also compared the $B(E2\uparrow)$'s for neutron-deficient Ge isotopes with the predictions of Hartree-Fock-Bogoliubov (HFB) calculations with configuration mixing performed via the generator coordinate method (GCM) treated in the Gaussian overlap approximation [45]. GCM is implemented with the technique of the five-dimension collective Hamiltonian (5DCH). The 5DCH calculations are performed with the Gogny D1S effective interaction [46,47] and the configuration mixing between the constrained HFB solutions exploring all quadrupole degrees of freedom. The observed trend of the $B(E2\uparrow)$'s is qualitatively reproduced even if the absolute values are 80% stronger than indicated by measurements. Overall, this model predicts too strong a collectivity for the $0_1^+ \rightarrow 2_1^+$ transition measured for the low-mass Ge isotopes.

B. Spectroscopy of ^{67}As

The γ-ray spectra of ^{67}As are shown in Fig. 5. The velocities used in the Doppler correction are $\beta = 0.385$ and 0.350 for Coulomb excitation and inelastic scattering, respectively. New transitions at 720(6) and 1242(9) keV have been observed in addition to the ones reported in Refs. [32,33] both in the Coulomb excitation and inelastic scattering channels. Hints of transitions at 639(6), 862(6), and 942(6) keV, already observed by Jenkins *et al.* and Orlandi *et al.* [32,33], have been observed in the inelastic channel only. Note that the transition at 862 keV is better Doppler corrected with $\beta = 0.360$. Both $\beta = 0.350$ and $\beta = 0.360$ correspond to an emission occurring in the second half of the target and, therefore, to the decay of states with a lifetime of the order of 10 ps. Other peaks that do not correspond to known transitions may be observed in the spectra of Fig. 5 but are not taken into account in this analysis because they are not observed in both rings of the SeGA array.

We investigated the spin-parity of the excited states by exploiting the selectivity of the Coulomb excitation mechanism and by comparison with shell-model calculations in the $f_{5/2}pg_{9/2}$ model space using the JUN45 interaction. Since the ground state is known to be $5/2^-$, an $E2$ excitation may reach

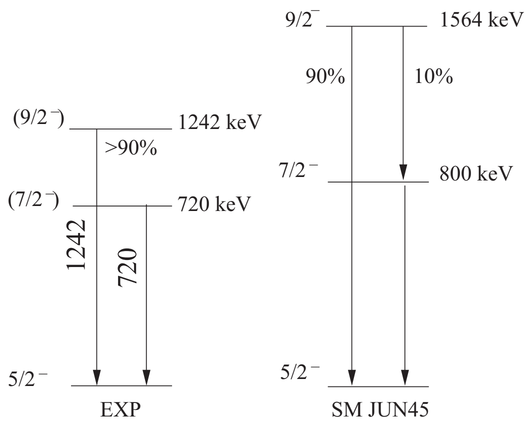

FIG. 6. (Color online) Proposed level scheme for ^{67}As. The new transitions observed in this measurement and the corresponding transitions obtained via a shell-model calculation with the JUN45 interaction are presented.

a final angular momentum of $3/2^-$, $5/2^-$, $7/2^-$, or $9/2^-$. The most likely spin-parity assignment is $7/2^-$, which is predicted by the shell model to be linked via the strongest E2 transition $[B(E2\uparrow; 5/2^- \to 7/2^-) = 1047\ e^2\text{fm}^4]$ to the ground state. We therefore propose the 720 keV transition as the $5/2^- \to 7/2^-$ excitation. The second strongest transition predicted by the shell model populates a $9/2^-$ state. No excited $9/2^-$ state has yet been observed in ^{67}As, while two have been observed in ^{69}As. We propose the 1242 keV transition as the decay from the $9/2^-$ to the ground state. The shell model predicts that the $9/2^-$ level decays with a branching ratio of 90% to the ground state and the remaining 10% to the $7/2^-$.

If such a transition were produced, we estimate that an amount of 40 counts or more at about 522 keV should be visible at both angular rings of the SeGA array. This limit of observation defines a conservative upper limit for the experimental branching ratio to the $7/2^-$ of 10%.

The proposed level scheme for the 720 keV and 1242 keV transitions is presented in Fig. 6, while a list of all observed transitions is given in Table II. The values $B(E2; 5/2_1^- \to 7/2_1^-)$ of 1162(236) $e^2\text{fm}^4$ and $B(E2; 5/2_1^- \to 9/2_1^-)$ of

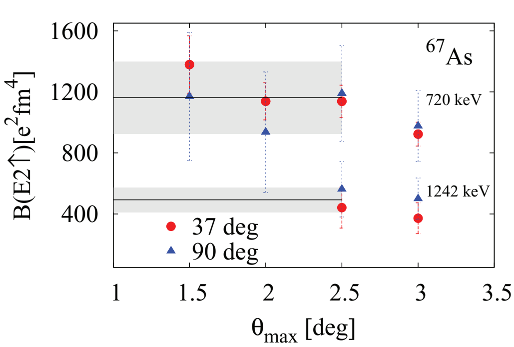

FIG. 7. (Color online) $B(E2\uparrow)$ transition probabilities for the $5/2_1^- \to 7/2_1^-$ and $5/2_1^- \to 9/2_1^-$ transitions in ^{67}As. The red and blue points correspond to the results obtained for the 37° and 90° ring with their statistical error. The black line corresponds to the average obtained considering the results up to 2.5°, and the shaded area represents the error on the average.

TABLE II. Energy of the transitions observed in coincidence with ^{67}As. The errors were obtained as the quadratic sum of the error of the fit, the error due to a 0.005 uncertainty on the value of β adopted in the Doppler correction, and a 4-keV error on the calibration.

J_i^π	E_{ex} (keV)	Transition	E_γ^{coulex} (keV)	$E_\gamma^{inelastic}$ (keV)
				639(6)
$7/2^-$	720(6)	$7/2^- \to 5/2^-$	720(6)	720(6)
				862(6)
				942(6)
$9/2^-$	1242(9)	$9/2^- \to 5/2^-$	1240(9)	1242(9)

460(70) $e^2\text{fm}^4$ were deduced considering scattering angles up to 2.5° (Fig. 7). If a 10% branching ratio for the $9/2_1^- \to 7/2_1^-$ decay is taken into account, a systematic error should be added to the statistical one, yielding estimates of $B(E2; 5/2_1^- \to 7/2_1^-) = 1162(236)(^{0}_{-90})\ e^2\text{fm}^4$ and $B(E2; 5/2_1^- \to 9/2_1^-) = 460(70)(^{+50}_{0})\ e^2\text{fm}^4$, respectively. The first value is in agreement with that from our shell model calculation, $B(E2; 5/2_1^- \to 7/2_1^-) = 1047\ e^2\text{fm}^4$, while the second one deviates by 1.3σ from the calculation, $B(E2; 5/2_1^- \to 9/2_1^-) = 379\ e^2\text{fm}^4$. This overall agreement gives additional credit to the spin-parity assignment.

One may wonder why the $7/2_1^-$ and $9/2_1^-$ states tentatively assigned here have not been observed in other experiments. The spectroscopy of ^{67}As produced using the fusion-evaporation technique is reported in Refs. [32,33]. The low-lying excited states were populated primarily from the decay of the higher-lying positive parity states, among which a $9/2^+$ state. According to shell-model calculations with JUN45 interaction, the occupancy of the $\nu g_{9/2}$ orbital is more than 2 for this state. The $g_{9/2}$ orbital has been already indicated as being responsible for the development of strong deformation in this region [49]. Conversely, low-lying negative-parity states have an occupancy of the $g_{9/2}$ orbital of less than 1, and smaller (in absolute value) quadrupole moments. The difference in structure of the positive- and negative-parity states may explain why this $7/2^-$ state was not populated via fusion evaporation. The values of the quadrupole moment for the $3/2_1^-$, $5/2_1^-$, $7/2_1^-$, and $9/2_1^-$ states in ^{67}As are plotted in Fig. 8(b), together with the ones of ^{65}As and ^{69}As.

As shown in Fig. 8(a), an inversion between the $5/2^-$ (predicted prolate) and the $3/2^-$ state (predicted oblate) excitation energies occurs between ^{65}As and ^{67}As, with the $3/2^-$ level becoming the ground state in ^{65}As. This inversion corresponds to a transition from a prolate to an oblate shape in the ground state, in line with the general trend observed in the region where oblate shapes appear close to the $N = Z$ line [31].

IV. STRUCTURE EVOLUTION THROUGH THE $^{64-72}$Ge ISOTOPES

A. Overall features

To shed more light on the structure of the $^{64-72}$Ge isotopes, the 5DCH model predictions are next challenged through

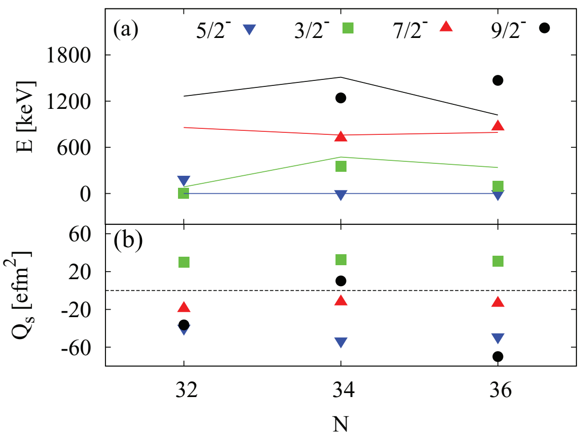

FIG. 8. (Color online) As isotopes with $32 \leqslant N \leqslant 36$. Experimental (symbols) and shell-model (lines) energies (a), and spectroscopic quadrupole moments (b) of the first low-lying negative-parity states. Shell model calculations are performed in the $f_{5/2}pg_{9/2}$ model space with the JUN45 interaction.

comparisons with measurements for *(i)* spectroscopic quadrupole moments, Q_s, of the first (2_1^+) and second (2_2^+) 2^+ states, *(ii)* $B(E2)$ between the 0_1^+, 2_1^+, and 2_2^+ levels, and *(iii)* odd-even staggering, $S(4)$, of the 2^+, 3^+, and 4^+ levels of the γ bands.

A first hint at structure properties is provided by inspecting the topology of potential energy surfaces (PESs) as shown in Figs. 9(a)–9(e). The PESs display evolution from rigid triaxial (^{64}Ge), to γ unstable (^{66}Ge), to soft triaxial (^{68,70,72}Ge). The red stars shown on the surfaces mark the mean β

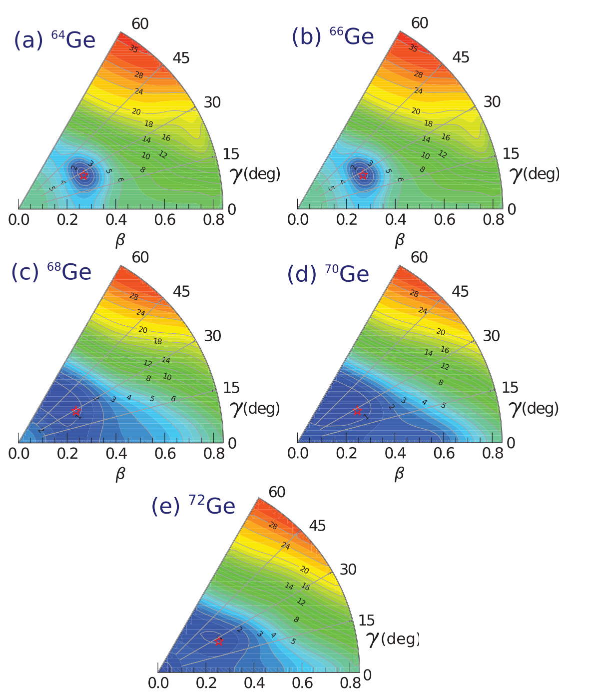

FIG. 9. (Color online) Potential energy surfaces from ^{64}Ge to ^{72}Ge calculated with the HFB model using the Gogny D1S interaction. Red stars mark mean β and γ deformations of the ground states.

and γ deformations, $\langle\beta\rangle$ and $\langle\gamma\rangle$, calculated for ground states. Values of $\langle\beta\rangle$ and $\langle\gamma\rangle$ are in the ranges $0.27 < \langle\beta\rangle < 0.29$ and $27^\circ < \langle\gamma\rangle < 29^\circ$. The PES properties together with those for mean deformations point to triaxial dynamical deformations. Softness is a common feature that is inferred from observing that the value of mean deformations $\langle\beta\rangle$ smoothly increases with angular momentum within a nucleus. Explicit treatment of the triaxial degree of freedom is essential to achieve a correct description of the structure within this mass region [7]. Other properties, namely the energy ratios $R_{42} = E(4_1^+)/E(2_1^+)$ and $R_{22} = E(2_2^+)/E(2_1^+)$ usually serve as structure indicators. Experimental values are taken from the Brookhaven data center [48]. The ratio R_{42}(exp) displays a smooth evolution from $R_{42}(\text{exp}) = 2.28$ (^{64}Ge) to $R_{42}(\text{exp}) = 2.07$ (^{70,72}Ge), suggesting a transition from γ-unstable ($R_{42} = 2.5$) to spherical shape ($R_{42} = 2$). The calculated ratios R_{42}(5DCH), though slightly higher, display a similar pattern and take on values ranging from $R_{42}(\text{5DCH}) = 2.64$ (^{64}Ge) to $R_{42}(\text{5DCH}) = 2.36$ (^{72}Ge). The second ratio, R_{22}, remains approximately constant for both data and present model calculations. R_{22}(exp) is approximately 1.75, except for ^{70}Ge where a lower value $R_{22}(\text{exp}) = 1.64$ is reached. From $N = 32$ to $N = 40$, the calculated ratios are $R_{22}(\text{5DCH}) = 2.02$, 2.12, 2.08, 1.98, and 2.02, values close to those expected from either the vibrational limit $R_{22} = 2$, or the asymmetric rotational model with γ deformation $\gamma = 30^\circ$. Again, a minimum in calculated energy ratios is observed for ^{70}Ge. Both data and calculations for R_{42} and R_{22} point to a complex structure evolution near and below $N = 40$ along the Ge isotopic chain. This minimum in 5DCH ratio predictions takes place even though $0^{+\prime}$ states intruding into the ^{70,72,74}Ge low-energy spectra—possibly of pairing vibration character [14]—lie outside the 5DCH framework.

Information on structure of nuclei in the Ge region as gained from features displayed by the ratios R_{42} and R_{22} is at most qualitative in nature. The property $R_{22}(\text{exp}) < 2$ is indicative of noncollective components present in the 2^+ wave functions.

B. Spectroscopic quadrupole moments

The measured and calculated Q_s values for the first (2_1^+) and second (2_2^+) 2^+ excited states are shown in Fig. 10(a). For rigid axially deformed nuclei considered in the rotational model [50], $Q_s(2_1^+)$ and $Q_s(2_2^+)$ values are expected to display identical magnitudes and opposite signs as long as the 2_2^+ level is a γ-band head. The same property, $Q_s(2_1^+) = -Q_s(2_2^+)$, holds based on the asymmetric rotational model [51]. For the Ge isotopes of present interest this condition is fulfilled: experimental [48] and calculated spectra display quasi-γ bands with the second 2^+ level as band head. As shown in Fig. 10(a), both Q_s values predicted in shell-model calculations with JUN45 (green solid and dashed curves) and 5DCH calculations (blue solid and dashed curves) generally are of opposite sign. We notice that the Q_s (2_1^+) and Q_s (2_2^+) values from 5DCH calculations display a negative sign for ^{70}Ge, and that both models globally predict $|Q(2_1^+)| \neq |Q(2_2^+)|$. The present model predictions do not match the available experimental Q_s values [48], nor are they complying with expectations for axial and triaxial rotational nuclei.

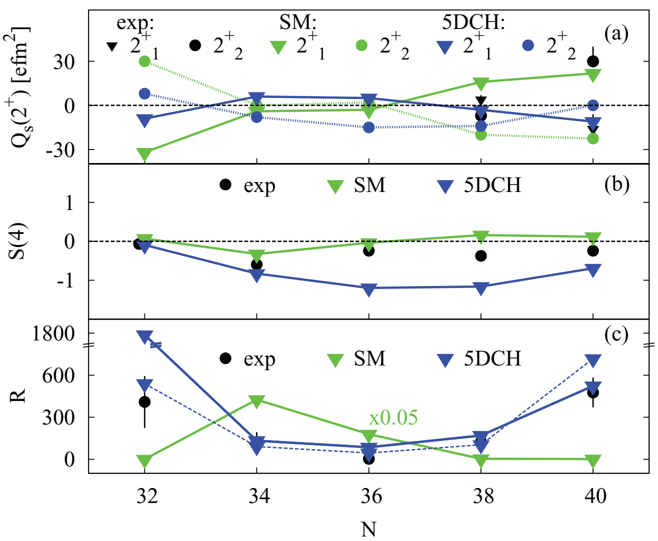

FIG. 10. (Color online) Comparison between experimental data and model predictions for $^{64-72}$Ge isotopes. (a) Spectroscopic quadrupole moments Q_s for the 2_1^+ and 2_2^+ levels, (b) staggering parameter $S(4)$, and (c) branching ratio $R = B(E2; 2_2^+ \to 2_1^+)/B(E2; 2_2^+ \to 0_1^+)$. Shell-model (5DCH) calculations are shown as green (blue) curves. In panel (c) the shell-model predictions are scaled by 0.05 for ease of comparison with data. For references to measurements see text. The dashed line in panel (c) is for 5DCH calculations using renormalized masses.

Previous shell model calculations based on the JUN45 and JJ4B interactions in the $f_{5/2}pg_{9/2}$ model space lead to similar conclusions, where limitations in the model space are suggested as the rationale for the fair success met with recent shell model predictions for spectroscopic quadrupole moments in Ge isotopes [52,53]. Effects of truncation in configuration spaces on predicted Q_s and $B(E2)$ values for the same isotopic chain have also been discussed within the interacting boson approximation (IBA-2) model [54]. In this publication the authors compared IBA-2 predictions based on calculations performed without and with consideration [15] of mixing between two structures coexisting inside a nucleus, in an attempt to explain coexistence phenomena observed near $N = 40$ [2]. It turns out that the predicted $Q_s(2^+)$ and $B(E2)$ values significantly depend upon whether configuration mixing is considered in IBA-2. This property here serves as an educated guess to make the point that dependence on configuration space of any of present model predictions for spectroscopic quadrupole moments is exacerbated whenever their values, including signs, are weak. In such a situation, the calculated $Q_s(2^+)$'s critically depend on details of the model wave functions.

C. Odd-even staggering

Whether γ-band properties are suggesting γ softness is investigated through considering the collective staggering parameter

$$S(4) = \{[E(4_2^+) - E(3_1^+)] - [E(3_1^+) - E(2_2^+)]\}/E(2_1^+),$$

where the 2^+, 3^+, and 4^+ levels are γ-band members [55–57]. The parameter $S(4)$ takes on the values $S(4) = -2$, $+0.33$, and -1 for γ-unstable, axially deformed, and vibrational nuclei, respectively. For the asymmetric rotational model, $S(4) = 5/3$ in the limit where the triaxial γ parameter is $\gamma = 30^\circ$ [57].

The experimental $S(4)_{\rm exp}$ values are inferred from the ENSDF database [48], except for ^{64}Ge. Here the ordering in the spin sequence 2^+, 3^+, and 4^+ is that suggested by shell-model predictions [29,44] and 5DCH results rather than that proposed on the basis of experimental data. Comparisons between $S(4)_{\rm exp}$ data and calculations are shown in Fig. 10(b). The $S(4)_{\rm exp}$ data (full dots) all show negative sign and absolute values smaller than unity. Neither present shell-model (green line) nor 5DCH (blue line) predictions match the data. The 5DCH values $S(4)_{\rm 5DCH}$ are all negative with $|S(4)_{\rm 5DCH}| < 1.2$ for $^{64-72}$Ge, suggesting a significant amount of γ softness. Except for ^{64}Ge and ^{66}Ge, the magnitude of calculated $S(4)$'s is stronger than that displayed by the $S(4)$ data.

D. $B(E2)$ ratio

A key indicator of structure evolution through the $^{64-72}$Ge isotopes is provided by the ratio $R = B(E2; 2_2^+ \to 2_1^+)/B(E2; 2_2^+ \to 0_1^+)$. Experimental $B(E2; 2_2^+ \to 2_1^+)$ and $B(E2; 2_2^+ \to 0_1^+)$ values are taken from [11] (^{64}Ge), [42] (^{66}Ge), [58] (^{68}Ge), [59] (^{70}Ge), and [60] (^{72}Ge). The experimental $B(E2)$ values entering the ratio R as a function of N do not display smooth patterns separately for the $2_2^+ \to 2_1^+$ and $2_2^+ \to 0_1^+$ transitions. However their ratios $R_{\rm exp}$, shown as full circles in Fig. 10(c), display an overall regular pattern. $R_{\rm exp}$ is at a maximum $R_{\rm exp} \sim 400$ for $N = 32$, next falls down and reaches the minimum $R_{\rm exp} = 1.7$ for $N = 36$, and rises up to reach $R_{\rm exp} \sim 500$ for $N = 40$.

The parabolic pattern shown by $R_{\rm exp}$ with increasing N calls for comments. We notice that the $B(E2; 2_2^+ \to 0_1^+)$ data never take on null values. The lowest $B(E2)$ values for this transition are seen for $N = 32$ and $N = 40$, which explain why $R_{\rm exp}$ reaches a maximum at the lower and higher N values. A conclusion based on $S(4)_{\rm exp}$ and $R_{\rm exp}$ properties is that between $N = 32$ and $N = 40$ the Ge isotopes behave as triaxial nuclei. Using words borrowed from the geometrical model picture, triaxial character is evolving from approximately rigid, to soft, and back to rigid over this N range.

The present shell-model predictions shown as a green curve in Fig. 10(c) are at odds in pattern and magnitude with the pattern displayed by the $R_{\rm exp}$ data. In contrast, the blue line standing for the 5DCH predictions is rather good in describing the overall experimental pattern. The ratio $R_{\rm exp}$ for ^{64}Ge is overestimated by a factor 4.5. This rapid change in the R systematics corresponds to the transition from a triaxial to a γ-soft shape observed in the PESs. Nevertheless, these latter predictions are consistent with data, again suggesting that Ge isotopes evolve from rigid to soft, and back to rigid "shapes."

E. Discussion

For many years 5DCH calculations were based on adopting the Inglis-Belyaev (IB) approximation for the determination of moments of inertia (MoI) and collective masses (CoMs), the two components of tensor of inertia. For calculating the MoI, a step forward has been accomplished in Ref. [45] where the IB approximation based on static HFB calculations has been removed and replaced by dynamical solutions obtained from rotating HFB mean-field calculations performed at very low rotational frequency ω, namely $\omega = 2$ keV. The outcome is a new MoI (see Eq. (8) in Ref. [45]) that here is labeled $\mathrm{MoI}_{\mathrm{TV}}$. $\mathrm{MoI}_{\mathrm{TV}}$ typically is larger than $\mathrm{MoI}_{\mathrm{IB}}$ by 30%. At this stage, $\mathrm{MoI}_{\mathrm{TV}}$ and $\mathrm{CoM}_{\mathrm{IB}}$ no longer fulfill minor symmetries specific to the collective Hamiltonian [61]. A step forward has next been taken aiming at restoration of these symmetries through renormalization of $\mathrm{CoM}_{\mathrm{IB}}$. For details, see Ref. [62]. The values taken by renormalized CoM, $\mathrm{CoM}_{\mathrm{Ren}}$, typically are stronger than $\mathrm{CoM}_{\mathrm{IB}}$ by 30%. The $\mathrm{CoM}_{\mathrm{Ren}}$ values are to be considered as approximations to actual CoMs. The main effect is found to lower energies of 0^+ excited states.

Here similar calculations are performed for the light Ge isotopes which are soft against triaxial deformations. Mass renormalization induces minor effects on the calculated ratios R_{42} and R_{22}. The R_{42}'s increase by 2% to 6%, implying that $^{64\text{–}72}$Ge keep similar their transitional characters. In contrast the R_{22}'s get lower in general. For example $R_{22} = 1.90$ (instead of $R_{22} = 2.02$ without renormalization) is the value calculated for ^{72}Ge. This lowering in R_{22}'s reflects minor changes in 5DCH predictions that also manifest in values taken by $\langle\beta\rangle$ and $\langle\gamma\rangle$ deformations separately attached to the 2_1^+ and 2_2^+ levels. Without mass renormalization, the ^{72}Ge mean deformations for the 2_1^+ and 2_2^+ states are $(\langle\beta\rangle_{2_1}, \langle\gamma\rangle_{2_1}) = (0.32, 26^\circ)$ and $(\langle\beta\rangle_{2_2}, \langle\gamma\rangle_{2_2}) = (0.34, 26^\circ)$. These values evolve to $(0.31, 27^\circ)$ and $(0.33, 26^\circ)$, respectively, once masses are renormalized. A difference $\delta\langle\beta\rangle$ is observed between the $\langle\beta\rangle$'s tied with the 2_1^+ and 2_2^+ levels. The value $\delta\langle\beta\rangle = 0.02$ is found stable under mass change. Its magnitude is too small for suggesting a kind of shape coexistence picture. Through mass renormalization, the calculated energy ratio R_{22} for Ge isotopes may reach lower values than without. Mass renormalization is not a clue for explaining why the experimental ratio R_{22}(exp) could be as low as $R_{22}(\mathrm{exp}) \sim 1.75$. Mass renormalization also induces minor alterations to calculated spectroscopic quadrupole moments and odd-even staggering parameters. There is no improvement in the predictions when comparison is made with those shown as blue curves in Figs. 10(a) and 10(b).

Significant progress in 5DCH predictions is achieved for the ratio R between the $B(E2; 2_2^+ \to 2_1^+)$ and $B(E2; 2_2^+ \to 0_1^+)$ rates. Effects of mass renormalization are the reduction and increase in the $B(E2; 2_2^+ \to 2_1^+)$ and $B(E2; 2_2^+ \to 0_1^+)$ strengths, respectively. The outcome is a lowering in the calculated R's, which is spectacular for ^{64}Ge. These predictions, shown as a blue dashed curve in Fig. 10(c), are closer to the R_{exp} data.

Finally, we notice that mass renormalization reduces the calculated $B(E2; 0_1^+ \to 2_1^+)$ strengths by approximately 10%, as shown by the dashed line in Fig. 4. This reduction is not strong enough to bring 5DCH predictions close to the $B(E2)$ data shown in Fig. 4. The results of present sensitivity calculations are encouraging. The hope is that improvements in 5DCH predictions for soft nuclei will be achieved once the tensor of inertia is established on solid microscopic grounds. An approach to this goal is based on the quasiparticle random phase approximation (QRPA) implemented with Gogny force [62].

V. CONCLUSIONS AND PERSPECTIVES

We reported on the spectroscopy of ^{66}Ge and ^{67}As via intermediate-energy Coulomb excitation, inelastic scattering, and one-proton knockout measurements. These probes offer different selectivity with respect to β-decay and fusion-evaporation production techniques.

We have measured a value of 1401(69) $e^2\mathrm{fm}^4$ for $B(E2; 0_1^+ \to 2_1^+)$ and set an upper limit of 50 $e^2\mathrm{fm}^4$ for $B(E2; 0_1^+ \to 2_2^+)$ in ^{66}Ge. The first value is in good agreement with that in Ref. [30], confirming the absence of a minimum in the $B(E2\uparrow)$ systematics as initially reported in Ref. [28]. We remark that the uncertainty on the $B(E2\uparrow)$'s obtained in this work is of the same order of magnitude as that obtained with the RDDS technique [30], confirming the degree of accuracy that one can achieve via intermediate-energy Coulomb excitation. Both shell-model calculations with the JUN45 interaction and 5DCH calculations with the Gogny D1S interaction overpredict the collectivity of the $0^+ \to 2_1^+$ transition in light Ge isotopes. A dominant soft-triaxial behavior is predicted by 5DCH calculations for light Ge isotopes, with ^{64}Ge and ^{72}Ge as the more rigid among them. Sensitivity calculations conducted within this model have shown that collective masses play a key role in modulating the strength of transitions between γ and yrast bands. CoMs stronger than those based on the cranking approximation help bringing 5DCH predictions closer to data. The outcome is viewed as an incentive for tailoring improved CoMs.

The γ-ray spectra measured for ^{67}As display new transitions. Tentative spin-parity assignments of $7/2^-$ and $9/2^-$ are proposed for the states decaying via the 720 and 1242 keV transitions, respectively, based on the selectivity of Coulomb excitation and comparison with shell-model calculations. $B(E2; 5/2_1^- \to 7/2_1^-) = 1162(236)(^{0}_{-90})$ $e^2\mathrm{fm}^4$ and $B(E2; 5/2_1^- \to 9/2_1^-) = 460(70)(^{+50}_{0})$ $e^2\mathrm{fm}^4$ have been deduced in ^{67}As. These values are in agreement with shell-model calculations with the JUN45 interaction.

Indirectly, this agreement gives credit to the shell-model predictions of a prolate shape for the ground state of ^{67}As, and rather spherical-prolate $(7/2_1^-)$ and spherical-oblate $(9/2_1^-)$ shapes for the excited states populated via Coulomb excitation. The complex structure of nuclei in this region, which is driven by a combination of collective and single particle effects, demands collecting more exclusive data to benchmark theoretical models. In this respect, measuring the g factor of the ^{67}As ground state would be a valuable asset.

$B(E2)$'s have been measured up to the $N = Z$ line via intermediate energy Coulomb excitation and lifetime measurements. They provide information on the collectivity and, in a model-dependent way, on the nuclear shape. The spectroscopic quadrupole moment is the only observable that directly probes the shape of the nuclear density distribution. It is very sensitive to the details of the shell-model wave function and therefore provides a critical test for microscopic model predictions. Since the only measurements allowing us to access this quantity are laser spectroscopy (for ground and isomeric states) and low-energy Coulomb excitation (for short-lived excited states), its value is experimentally determined only for the less exotic isotopes of the region. Namely, the quadrupole moments and $E2$ transition probability have been measured for $N \geqslant 38$ for Ge and Kr isotopes, and $N \geqslant 36$ for Se isotopes. The measurement of quadrupole moments of, and $E2$ transition rates between, low-lying states in $N \sim Z$ nuclei, primarily ^{66,68}Ge isotopes, remains an experimental challenge for existing and upcoming low-energy radioactive-beam facilities. Low-lying 0^+ states have already provided a signature of shape coexistence in ^{74,76}Kr and of a configuration transition between ^{72}Ge and ^{70}Ge. Such 0^+ states are predicted by shell-model calculations for several nuclei in the region, including ^{66}Ge, ^{66}Se, and ^{70}Se, but have not yet been observed. Two-neutron transfer reactions, which are selective with respect to 0^+ states, may be a suitable probe.

The shell model with the JUN45 interaction together with the 5DCH model with the D1S force have each shown limitations in their respective predictive power. The problem seems rooted in an insufficient size of the configuration space. Recent shell-model extensions [63] may lead to improved predictions for Ge isotopes of present interest. In contradistinction, the inclusion of pairing vibrations seems beyond the reach of 5DCH. Instead, advances are expected from the multiparticle-multihole configuration mixing method [64,65], where the former dichotomy between collective and quasiparticle degrees of freedom at play in configuration space is no longer a prerequisite. This approach, based on the Gogny density functional, treats any excited level in a nucleus as a multiparticle-multihole excitation and provides multipole transition rates free of effective charge. Our hope is that this new-generation structure model will improve the understanding of the complex properties of nuclei in the $A \sim 70$ mass region.

ACKNOWLEDGMENTS

This work was partially supported by the National Science Foundation under Grant No. PHY-0606007. A.C. acknowledges the support of the CEA-EUROTALENTS program.

[1] P. Cejnar, J. Jolie, and R. F. Casten, Rev. Mod. Phys. **82**, 2155 (2010).
[2] K. Heyde and J. L. Wood, Rev. Mod. Phys. **83**, 1467 (2011).
[3] E. Bouchez *et al.*, Phys. Rev. Lett. **90**, 082502 (2003).
[4] E. Clément *et al.*, Phys. Rev. C **75**, 054313 (2007).
[5] A. M. Hurst *et al.*, Phys. Rev. Lett. **98**, 072501 (2007).
[6] J. Ljungvall *et al.*, Phys. Rev. Lett. **100**, 102502 (2008).
[7] M. Girod, J.-P. Delaroche, A. Gorgen, and A. Obertelli, Phys. Lett. B **676**, 39 (2009).
[8] K. Sato and N. Hinohara, Nucl. Phys. A **849**, 53 (2011).
[9] A. Obertelli *et al.*, Phys. Rev. C **80**, 031304 (2009).
[10] A. Lemasson *et al.*, Phys. Rev. C **85**, 041303 (2012).
[11] K. Starosta *et al.*, Phys. Rev. Lett. **99**, 042503 (2007).
[12] M. Sugawara *et al.*, Eur. Phys. J. A **16**, 409 (2003).
[13] B. Kotlinski, T. Czosnyka, D. Cline, J. Srebrny, C. Wu, A. Backlin, L. Hasselgren, L. Westerberg, C. Baktash, and S. Steadman, Nucl. Phys. A **519**, 646 (1990).
[14] K. J. Weeks, T. Tamura, T. Udagawa, and F. J. W. Hahne, Phys. Rev. C **24**, 703 (1981).
[15] P. Duval, D. Goutte, and M. Vergnes, Phys. Lett. B **124**, 297 (1983).
[16] M. Didong, H. Müther, K. Goeke, and A. Faessler, Phys. Rev. C **14**, 1189 (1976).
[17] K. Kumar, J. Phys. G **4**, 849 (1978).
[18] A. van den Berg, R. Janssens, G. Emery, A. Saha, and R. Siemssen, Nucl. Phys. A **379**, 239 (1982).
[19] A. Becker, C. Alderliesten, E. Bakkum, K. V. D. Borg, C. V. Engelen, L. Zybert, and R. Kamermans, Nucl. Phys. A **388**, 477 (1982).
[20] A. Petrovici, K. Schmid, F. Grummer, A. Faessler, and T. Horibata, Nucl. Phys. A **483**, 317 (1988).
[21] J. P. Bazantay *et al.*, Phys. Rev. Lett. **54**, 643 (1985).
[22] K. Takada and S. Tazaki, Nucl. Phys. A **448**, 56 (1986).
[23] V. G. Pedrocchi and T. Tamura, J. Phys. G **14**, 321 (1988).
[24] L. Chaturvedi *et al.*, Phys. Rev. C **43**, 2541 (1991).
[25] S. T. Hsieh, H. C. Chiang, and D.-S. Chuu, Phys. Rev. C **46**, 195 (1992).
[26] J. Joubert, F. J. W. Hahne, P. Navrátil, and H. B. Geyer, Phys. Rev. C **50**, 177 (1994).
[27] A. Petrovici, K. Schmid, A. Faessler, J. Hamilton, and A. Ramayya, Prog. Part. Nucl. Phys. **43**, 485 (1999).
[28] R. Wadsworth, L. P. Ekstrom, G. D. Jones, F. Kearns, T. P. Morrison, O. M. Mustaffa, H. G. Price, P. J. Twin, and N. J. Ward, J. Phys. G **5**, 1761 (1979).
[29] M. Honma, T. Otsuka, T. Mizusaki, and M. Hjorth-Jensen, Phys. Rev. C **80**, 064323 (2009).
[30] R. Lüttke *et al.*, Phys. Rev. C **85**, 017301 (2012).
[31] A. Obertelli *et al.*, Phys. Lett. B **701**, 417 (2011).
[32] D. G. Jenkins *et al.*, Phys. Rev. C **64**, 064311 (2001).
[33] R. Orlandi *et al.*, Phys. Rev. Lett. **103**, 052501 (2009).
[34] P. Baumann *et al.*, Phys. Rev. C **50**, 1180 (1994).
[35] P. G. Hansen and J. A. Tostevin, Annu. Rev. Nucl. Part. Sci. **53**, 219 (2003).
[36] T. Glasmacher, Annu. Rev. Nucl. Part. Sci. **48**, 1 (1998).
[37] J. O. Newton, in *The Electromagnetic Interaction in Nuclear Spectroscopy*, edited by W. D. Hamilton (North Holland, Amsterdam, 1975), pp. 237–282.
[38] D. Bazin, J. Caggiano, B. Sherrill, J. Yurkon, and A. Zeller, Nucl. Instrum. Methods B **204**, 629 (2003).
[39] W. Mueller, J. Church, T. Glasmacher, D. Gutknecht, G. Hackman, P. Hansen, Z. Hu, K. Miller, and P. Quirin, Nucl. Instrum. Methods A **466**, 492 (2001).
[40] D. Morrissey, B. Sherril, M. Steiner, and A. Stolz, Nucl. Instrum. Methods B **204**, 90 (2003).
[41] A. Winther and K. Alder, Nucl. Phys. A **319**, 518 (1979).
[42] E. Browne and J. Tuli, Nucl. Data Sheets **111**, 1093 (2010).
[43] M. Honma, T. Otsuka, B. A. Brown, and T. Mizusaki, Phys. Rev. C **69**, 034335 (2004).
[44] M. Hasegawa, K. Kaneko, and T. Mizusaki, Phys. Rev. C **70**, 031301 (2004).

[45] J.-P. Delaroche, M. Girod, J. Libert, H. Goutte, S. Hilaire, S. Péru, N. Pillet, and G. F. Bertsch, Phys. Rev. C **81**, 014303 (2010).
[46] J. Dechargé and D. Gogny, Phys. Rev. C **21**, 1568 (1980).
[47] J. Berger, M. Girod, and D. Gogny, Comput. Phys. Commun. **63**, 365 (1991).
[48] ENSDF database, http://www.nndc.bnl.gov/ensdf/
[49] B. Heits, H.-G. Friederichs, A. Gelberg, K. Lieb, A. Perego, R. Rascher, K. Zell, and P. V. Brentano, Phys. Lett. B **61**, 33 (1976).
[50] A. Bohr and B. R.Mottelson, *Nuclear Structure,* Vol. II (W. A. Benjamin, Reading, MA, 1975).
[51] A. Davydov and G. Filippov, Nucl. Phys. **8**, 237 (1958).
[52] S. J. Q. Robinson, L. Zamick, and Y. Y. Sharon, Phys. Rev. C **83**, 027302 (2011).
[53] G. Gürdal *et al.*, Phys. Rev. C **88**, 014301 (2013).
[54] S. Brant, N. Yoshida, and L. Zuffi, Phys. Rev. C **70**, 054301 (2004).
[55] N. Zamfir and R. Casten, Phys. Lett. B **260**, 265 (1991).
[56] E. A. McCutchan *et al.*, Phys. Rev. C **76**, 064307 (2007).
[57] R. F. Casten, *Nuclear Structure from a Simple Perspective*, Oxford Studies in Nuclear Physics No. 23 (Oxford University Press, Oxford, 2000).
[58] J. Leske, K.-H. Speidel, S. Schielke, O. Kenn, J. Gerber, P. Maier-Komor, S. J. Q. Robinson, A. Escuderos, Y. Y. Sharon, and L. Zamick, Phys. Rev. C **71**, 044316 (2005).
[59] J. Leske, K.-H. Speidel, S. Schielke, J. Gerber, P. Maier-Komor, S. J. Q. Robinson, A. Escuderos, Y. Y. Sharon, and L. Zamick, Phys. Rev. C **74**, 024315 (2006).
[60] D. Abriola and A. Sonzogni, Nucl. Data Sheets **111**, 1 (2010).
[61] K. Kumar and M. Baranger, Nucl. Phys. A **92**, 608 (1967).
[62] J. Libert, J.-P. Delaroche, M. Girod, H. Goutte, S. Hilaire, S. Peru, N. Pillet, and G. F. Bertsch, J. Phys.: Conf. Ser. **205**, 012007 (2010).
[63] S. M. Lenzi, F. Nowacki, A. Poves, and K. Sieja, Phys. Rev. C **82**, 054301 (2010).
[64] N. Pillet, J.-F. Berger, and E. Caurier, Phys. Rev. C **78**, 024305 (2008).
[65] N. Pillet, V. G. Zelevinsky, M. Dupuis, J.-F. Berger, and J. M. Daugas, Phys. Rev. C **85**, 044315 (2012).